

Supporting Information

Grotto Microenvironment Shapes Aerosol Composition: Implications for Long-Term Preservation of Stone Carvings

Yajuan Yang^{a,b}, Hong Geng^{a,b,*}, Li Wu^a, Runping Zhang^c, Hongbin Yan^c, Shangxiao Qiao^c, Daizhou Zhang^d, Liangliang Hou^{b,e}, Jianhui Zhi^f

^a Institute of Environmental Science, Shanxi University, Taiyuan 030031, China

^b The Joint School of Graduate Studies in Grotto Culture in China, Taiyuan 030006, China

^c Shanxi Key Laboratory of Grotto Temple Protection and Inheritance, Yungang Academy, Datong 037007, China

^d Faculty of Environmental and Symbiotic Sciences, Prefectural University of Kumamoto, Kumamoto 862-8502, Japan

^e College of Archaeology and Museology, Shanxi University, Taiyuan 030006, China

^f College of Environmental & Resource Sciences, Shanxi University, Taiyuan 030031, China

* Corresponding author. Tel.: +86 15003439409

E-mail address: genghong@sxu.edu.cn (H. Geng)

Number of pages of text: 1

Number of tables: 2

Number of figures: 4

This supporting information document contains the following information:

- Supplemental Text

Text S1. Identification rules and morphological characteristics of different types of particles based on low-Z particle EPMA analysis

- Supplemental Tables

Table S1. Sampling times and meteorological conditions

Table S2. Classification rules of individual particles based on their morphological and X-ray spectral characteristics

- Supplemental Figures

Figure S1. X-ray spectra and elemental atomic concentrations calculated through Monte Carlo simulation for typical mineral dust particles.

Figure S2. X-ray spectra and elemental atomic concentrations calculated through Monte Carlo simulation for typical sodium salt particles.

Figure S3. X-ray spectra and elemental atomic concentrations calculated through Monte Carlo simulation for other particles.

Figure S4. 48 h backward trajectories of air masses.

Figure S5. Comparison of atomic concentration of S and N for RMD.

- * **Supplemental Text (including references)**

Text S1. Identification rules and morphological characteristics of different types of particles based on low-Z particle EPMA

(1) Carbonaceous particles

The EC or carbon-rich particles, generated from complete or incomplete combustion (oil, coal, and biomass burning or smoldering), were further classified into three sub-types. The first is tar balls, which have bright, spherical shapes (Fig. 4c). The second type is char, exhibiting an irregular shape and gray color (Fig. S1a). The third is soot, the chain-like agglomerates of primary spherical carbon from gasoline or diesel combustion (Fig. S1b).

The OC particles were roughly classified into two sub-types, *i.e.* water-soluble and

insoluble organic carbon (WSOC and WIOC), without large difference in concentrations of C and O. Some appear bright and irregular, and some appear as dark droplets (Fig. 4a-c). The frequently encountered particles are the ones with round or oval shapes and smooth surfaces, e.g., particles #94 in Fig. 3e. They are often enclosed by light-dark water-like or colloidal matter.

(2) Unreacted Mineral dust (UMD) and Reacted Mineral dust (RMD)

Mineral dust, which usually has a bright and irregular morphology, includes aluminosilicate (AlSi-containing particles), SiO_2 , CaCO_3 , TiO_2 , and MgCO_3 or other Fe-containing species, as shown in Fig. 4a-c. Silicate-containing particles that have been reacted with airborne SO_2 and NO_x or with the “secondary acids” (nitric or sulfuric acids) in the atmosphere were usually a complex mixture with multiple elements, including Al, Si, O, Ca, Mg, K, Na, S, and N. They are easily identified owing to their characteristic elements of Al and Si with liquid-like shade surrounding them on their SEIs and with N or S peaks in their X-ray spectra, which are named as RMD.

(3) Sodium salt particles

Pure NaCl particles are mostly regular cubes with sharp edges, smooth surfaces, and a Na/Cl molar ratio close to 1:1, with few impurities; Na_2SO_4 particles present plate-like or flocculent aggregates with blunt edges, characterized by the core elements Na, S, and O in a molar ratio of approximately 2:1:4 and no Cl element; S/N-NaCl particles retain the cubic morphology of NaCl but have rough surfaces covered with a thin S/N-containing coating; Halite particles are irregular morphology and Na/Cl as the main elements accompanied by impurity elements such as Ca, Mg, and Si; S/N-Halite

particles take natural Halite as the core, with S/N-containing substances attached to the surface and pores.

(4) Others

The O-rich, TiO₂, CNOS-containing (secondary particles), K₂SO₄, biological particles, etc., with low abundances of 1.2–2.0%, are classified into “others”. The O-rich, TiO₂, KCl, and K₂SO₄ particles have a bright and irregular morphology. The biogenic particles are generally identified based on their unique morphology and the presence of C, N, O, K, P, S, and Cl peaks in their X-ray spectra. The CNOS-containing particles, which are composed solely of C, N, O, and S peaks in their X-ray spectra, potentially the mixture of water-soluble organic matter with secondary particles, are crucial tracers for evaluating atmospheric aging processes. These particles typically manifest as black liquid droplets encapsulating white, incompletely reacted cores. When probed by elemental analysis beams, they often exhibit characteristic perforations or “black holes” (Fig. S3a).

*** Supplemental Tables:**

Table S1 Sampling times and meteorological conditions.

Date	Sampling		Stage	Direction	Wind	T	RH	PM _{2.5}
	Time (UTC+8)	Location			Speed (m·s ⁻¹)	(°C)	(%)	μg·m ⁻³
Jan. 11, 2024	17:36-18:27	Site 3	$\frac{\text{St 2}}{\text{St 3}}$	EES	1.3	2.4	37.4	45.3
	19:10-19:46	Site 2	$\frac{\text{St 2}}{\text{St 3}}$	ES-E	0.5	1.2	42.5	37.2
	20:00-21:33	Site 1	$\frac{\text{St 2}}{\text{St 3}}$	S	0	-2.8	60.8	40.7
Jan. 12, 2024	8:45-9:25	Site 3	$\frac{\text{St 2}}{\text{St 3}}$	EES	0.4	6.2	24.6	54.4
	11:35-12:14	Site 2	$\frac{\text{St 2}}{\text{St 3}}$	ESS	0.1	6.5	30.0	49.4
	12:27-13:07	Site 1	$\frac{\text{St 2}}{\text{St 3}}$	Calm	0	1.1	36.5	45.0
	14:35-15:23	Site 3	$\frac{\text{St 2}}{\text{St 3}}$	EN	1.2	15.1	20.2	26.4
	16:47-17:14	Site 2	$\frac{\text{St 2}}{\text{St 3}}$	E	0.5	10.1	24.8	77.6
	17:35-18:15	Site 1	$\frac{\text{St 2}}{\text{St 3}}$	Calm	0	0.2	45.0	74.5

Jan. 13, 2024	8:40-9:17	Site 3	$\frac{\text{St 2}}{\text{St 3}}$	W-EN	1.5	-4.1	46.0	76.3
	9:55-10:33	Site 2	$\frac{\text{St 2}}{\text{St 3}}$	EEN-E	0.6	-3.7	52.6	75.6
	10:44-11:24	Site 1	$\frac{\text{St 2}}{\text{St 3}}$	Calm	0	-2.5	49.8	77.3
	16:42-17:32	Site 3	$\frac{\text{St 2}}{\text{St 3}}$	EN	0.7	3.5	41.3	68.3
	19:25-20:02	Site 2	$\frac{\text{St 2}}{\text{St 3}}$	ES	0.5	-2.8	61.4	31.4
	20:13-20:53	Site 1	$\frac{\text{St 2}}{\text{St 3}}$	Calm	0	-0.7	55.8	19.9
Jan. 14, 2024	7:28-8:08	Site 3	$\frac{\text{St 2}}{\text{St 3}}$	WS	0.5	-15.0	18	12.0
	8:26-9:13	Site 2	$\frac{\text{St 2}}{\text{St 3}}$	WWS	0.5	-10.0	20	10.0
	9:20-11:45	Site 1	$\frac{\text{St 2}}{\text{St 3}}$	Calm	0	-5.6	57.2	14.5

Table S2 Classification rules of individual particles based on their morphological and X-ray spectral characteristics.

Group	Particle types	Characteristics of SEM images and X-ray spectral data
1 Carbonaceous particles	Char, soot & tar ball	The sum of the C and O concentration is >90 at.%, in which the concentration of C is much larger (generally >3 times) than that of O, and almost no other element is present. Soot aggregates, tar ball (round shapes), and char irregular shapes are included
	OC	Irregular and solid particles, or dark droplets, with >90 at.% of C, O, and sometimes N (concentration of C is not much larger than that of O)
2. Unreacted (or primary) mineral dust (UMD)	SiOx & FeOx	Irregular shapes with strong Si or Fe and O signals in their X-ray spectra (the atomic concentration ratio of Si and O is around 1:2. FeOx particles have irregular shapes on SEI and usually contain more than 20 at.% Fe)
	CaCO ₃ & CaMg(CO ₃) ₂	Irregular shapes with strong C, O, Ca and/or Mg signals in their X-ray spectra

	Aluminosilicate (AlSiO _x , K-AlSiO _x , Ca-AlSiO _x , Na-AlSiO _x , Mg-AlSiO _x , Fe-AlSiO _x ,)	Irregular shapes with strong Al, Si, and O peaks in their X-ray spectra, often with other elements, such as Na, Mg, K, Ca, and Fe, the richest element named element -AlSiO _x .
3. Reacted mineral dust (RMD)	Aged or reacted aluminosilicate, SiO ₂ , CaCO ₃ , CaMg(CO ₃) ₂ , etc. (Some of them are reacted with SO _x and NO _x or H ₂ SO ₄ and HNO ₃ ; some of them are enclosed or mixed with (NH ₄) ₂ SO ₄ and/or NH ₄ NO ₃)	Irregular shapes often with dark droplet being enclosed or mixed, having N and/or S peaks in X-ray spectra (indicative of either nitrates, sulfates, or both on their surfaces)
4. Sodium salt particles	NaCl, Na ₂ SO ₄ , S/N-NaCl, Halite particles, S/N- Halite particles	Cubic shapes with predominant Na and Cl signals and minor C, O, Mg, and etc. in X-ray spectra; Cubic or round shapes with droplets covered or enclosed, containing N and/or S besides O, Na and Cl, sometimes with detectable Al, Si, C, K, Ca, Mg and Fe
5. Others	Biological particles, O-rich, K ₂ SO ₄ , CNOS, et	Most of them are irregular and bright in shape. Biological particles have

	al.	round shells or surfaces and often contain elements that make up biological organisms such as K, N, C, O and S. And the CNOS-containing particles are regarded as the secondary particles containing organic matter, $(\text{NH}_4)_2\text{SO}_4/\text{NH}_4\text{HSO}_4$, and perhaps NH_4NO_3 .
--	-----	--

* Supplemental Figures:

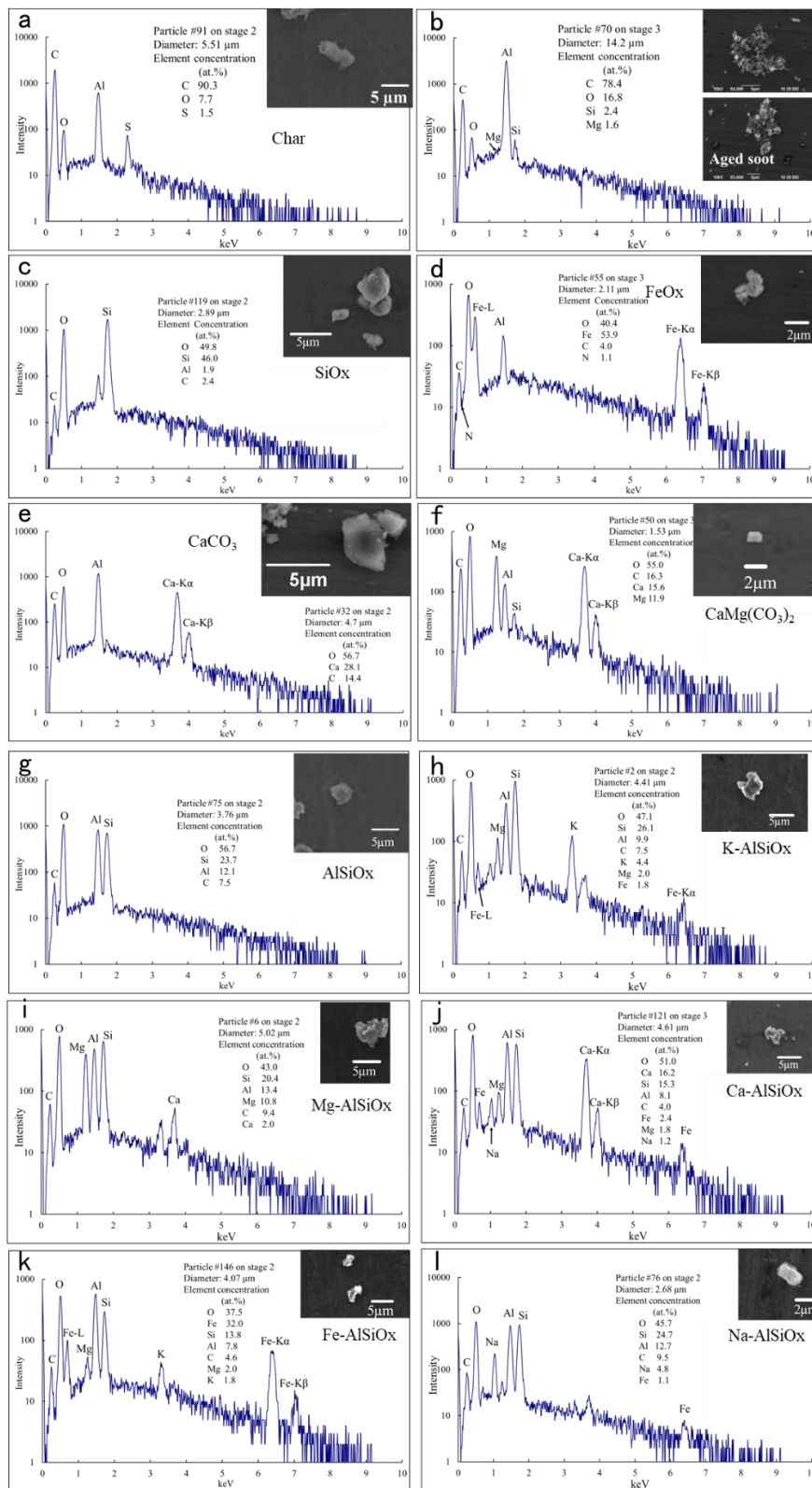


Figure S1. X-ray spectra and elemental atomic concentrations calculated through Monte Carlo simulation for typical mineral dust particles.

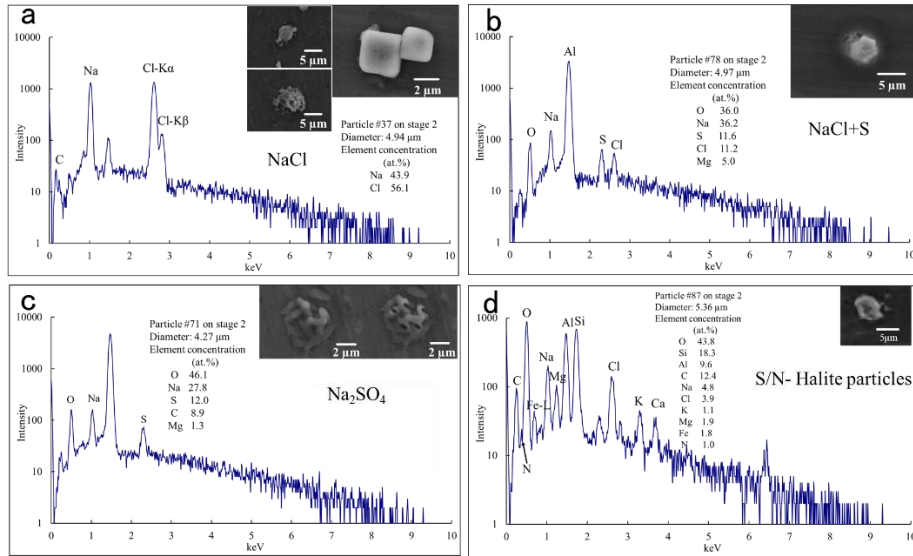


Figure S2 X-ray spectra and elemental atomic concentrations calculated through Monte Carlo simulation for typical sodium salt particles.

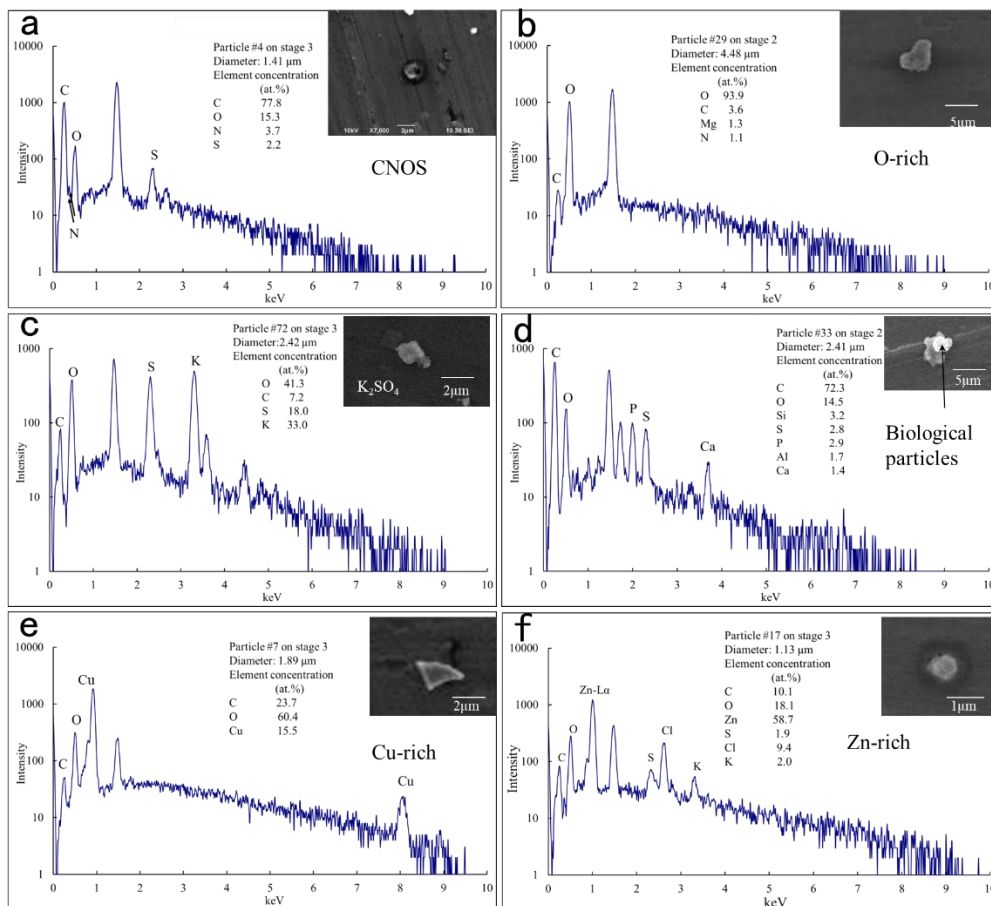


Figure S3 X-ray spectra and elemental atomic concentrations calculated through Monte Carlo simulation for other particles.

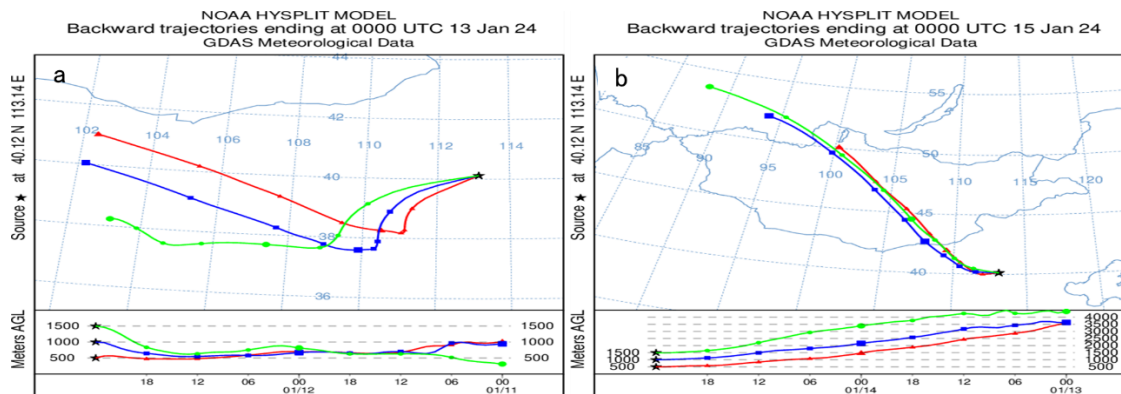


Figure S4. The 48 h backward air mass trajectories at receptor heights of 500 m, 1000 m, and 1500 m (Above Ground Level) were produced using the HYbrid Single-Particle Lagrangian Integrated Trajectory model available at the NOAA Air Resources Laboratory's web server (<http://ready.arl.noaa.gov/HYSPLIT.php>). (a) at 0:00UTC on 13 January 2024; (b) at 0:00UTC on 15 January 2024.

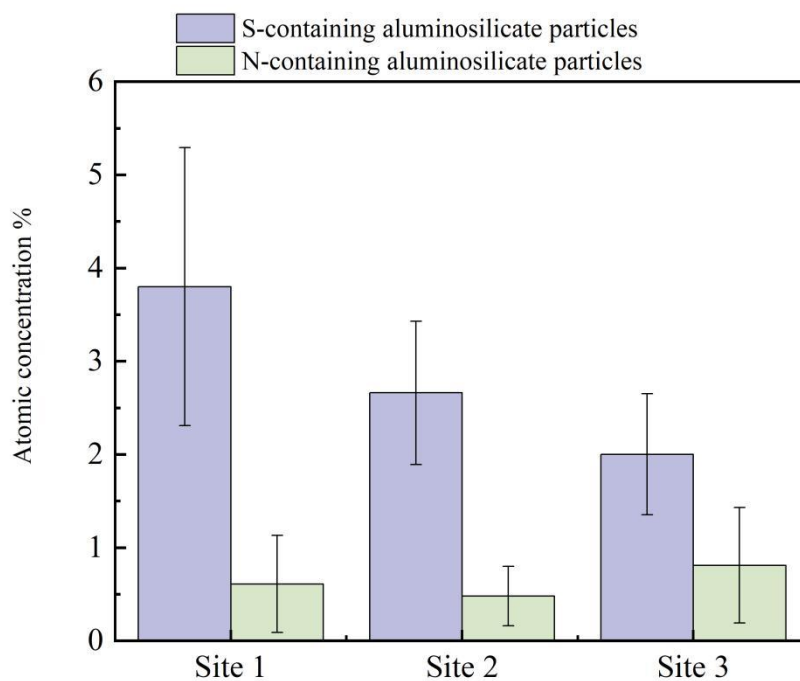


Figure S5. Atomic concentration of S and N in RMD.